Input Conductance of a Four-Frequency Parametric Up-Converter

A. KORPEL AND V. RAMASWAMY, MEMBER, IEEE

Abstract—The limited power gain of a parametric upper sideband up-converter may be enhanced arbitrarily by allowing additional dissipation of energy at the lower sideband. However, the input conductance of such a four-frequency device will be critically dependent upon the amount of lower sideband energy dissipated. In this paper, we shall consider a varactor diode-type four-frequency up-converter employing a single resonant circuit common to both the pump and the sidebands. The input conductance of this configuration is analyzed in terms of the relative deviation of the pump frequency from the resonance frequency of the common circuit. We show that the input conductance also is seriously affected by the presence of second harmonic capacitance variation such as may occur at high-pump levels. Numerical results have been plotted for a wide range of circuit parameters. Also presented in this paper are the experimental results of measurements performed on such an amplifier, showing good agreement with the theory.

Introduction

IT IS WELL KNOWN that diode parametric amplifiers, in general, exhibit considerable complexity in circuitry and evidence severe stability problems. An exception to this is the upper sideband up-converter which is unconditionally stable by virtue of its positive input conductance. However, its conversion gain is limited to the ratio of the upper sideband frequency to the input frequency. It has frequently been pointed out that the inclusion of the lower sideband makes it possible to achieve higher conversion gain while maintaining a positive input conductance [1]–[5]. In general, the value of the input conductance is determined by the relative loading of the two sidebands and actually will become negative if the ratio of the energy dissipated in the lower sideband to that in the upper sideband exceeds the ratio of their frequencies. To achieve high-conversion gain, it is necessary to operate close to this limit.

The simplest way to achieve such high-gain operation is to use a single resonant circuit tuned to the pump frequency. This provides equal loading for both sidebands and, as seen later, a conversion gain equal to the square of the pump to signal frequency ratio. Amplifiers of this kind have been reported by Adams and Brett, et al., and were designed as phase-shift amplifiers [6], and standing-wave amplifiers [7], etc. In such amplifiers, the ratio of energy dissipated in the lower sideband to that in the upper sideband equals the square of the ratio of the two frequencies. Usually, this is close to unity and, therefore, close to the critical ratio previously mentioned. Consequently, the stability of such an amplifier would seem to depend, rather critically, on any change in pump power or frequency, through the resulting variations in the input conductance.

On the other hand, this particular dependence may be put to use in the simple circuit mentioned earlier, i.e., one may vary the ratio of the energy dissipated in the lower sideband to that in the upper sideband and, hence, the input conductance by simply detuning the pump or the resonant circuit. This flexibility should make it possible to meet different bandwidth and gain requirements in a simple way by selecting a mode of operation somewhere between an upper sideband and a lower sideband up-converter.

The above-mentioned considerations were thought to be of sufficient importance to warrant a detailed theoretical and experimental investigation into the behavior of the input conductance of a four-frequency parametric device using a single resonant circuit common to both idlers and pump.

The relevant parameters considered in this paper are the relative deviation of the pump frequency, the input frequency, and the pump level. The first two quantities are normalized with respect to the bandwidth of the pump circuit; the input conductance is normalized with respect to a quantity involving the first harmonic capacitance variation, thus implicitly showing the first-order dependence on the pump level.

As will be seen, the effect of second harmonic capacitance variation becomes very important for higher pump levels. It introduces a coupling between the sidebands, and thus considerably affects the input conductance. This enters into the expression as a simple "feedback" parameter. Another effect of this second harmonic capacitance variation is to modify the effective average capacitance seen by the sidebands so as to coincide with the large signal capacitance seen by the pump. Moreover, the second harmonic capacitance variation defines a region of instability (ferroresonant or jump effect) in which the theoretical expressions do not have practical meaning.

Experiments performed on a typical circuit are described toward the end of the article and the results compared with the theoretical values.

General Relations for Input Conductance and Conversion Gain

Figure 1 shows the relevant parameters pertaining to a generalized representation of a four-frequency parametric device. The frequencies involved are ω_1, the sig-

Manuscript received June 11, 1964; revised September 23, 1964.
The authors are with the Zenith Radio Corporation, Chicago, Ill.

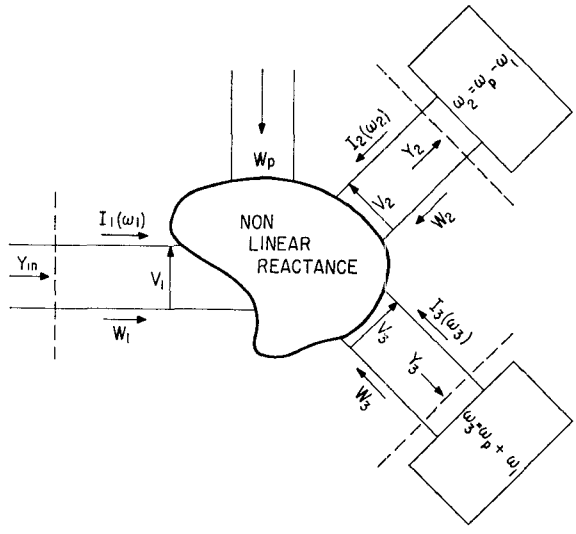

Fig. 1. Basic representation of four-frequency parametric device.

nal frequency; ω_p, the pump frequency; ω_2 and ω_3, the lower and upper sideband frequencies. The sideband loading is represented by admittances Y_2 and Y_3, while Y_{in} denotes the input admittance. Note that Y_{in} refers to the input admittance reflected by the nonlinear element only, and does not include any other external admittances at the input circuit. The nonlinear reactance coupling the various frequencies is assumed to satisfy the Manley-Rowe relations, but otherwise is not specified at this point. Powers (W), voltages (V), and currents (I) at the frequencies of interest are shown in the figure. Powers are taken to be positive if flowing into the nonlinear reactance.

As first stated by Manley and Rowe [8], the basic energy relations for such a configuration as in Fig. 1 are given by

$$\frac{W_3}{\omega_3} - \frac{W_2}{\omega_2} + \frac{W_1}{\omega_1} = 0 \tag{1}$$

$$\frac{W_p}{\omega_p} + \frac{W_3}{\omega_3} + \frac{W_2}{\omega_2} = 0 \tag{2}$$

The second relation involving the pump power is equivalent to a conservation of energy statement. Inasmuch as the pump power is not considered here, this relation need not concern us.

The conversion gain is defined on the basis of power delivered to the sideband loads as

$$G_c = -\frac{(W_2 + W_3)}{W_1} \tag{3}$$

With (1), this may be written as

$$G_c = \frac{\omega_2}{\omega_1} \frac{1 + (W_2/W_3)}{(\omega_2/\omega_3) - (W_2/W_3)} \tag{4}$$

The input admittance Y_{in} may be written as

$$Y_{in} = G_{in} + B_{in} \tag{5}$$

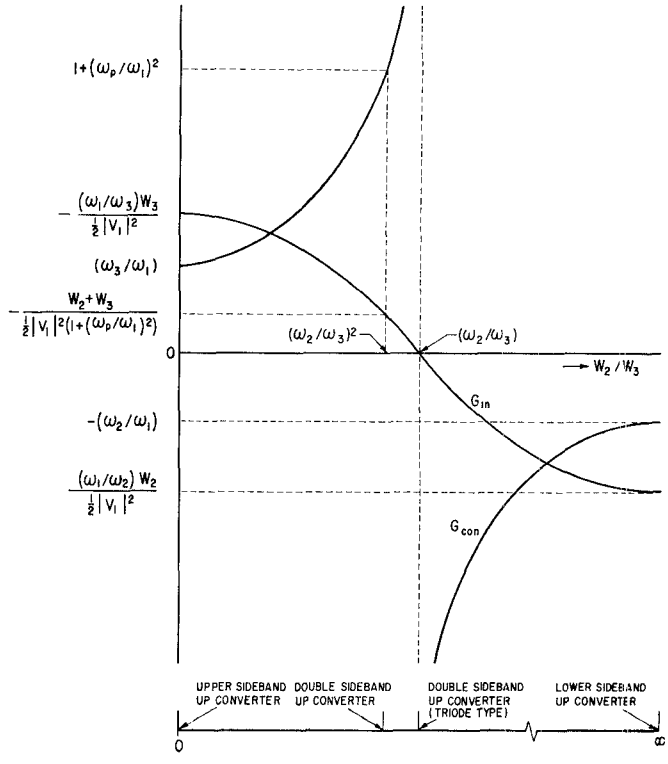

Fig. 2. Conversion gain and input conductance for various modes of operation of four-frequency parametric devices.

and

$$W_1 = 1/2\,|V_1|^2 G_{in} \tag{6}$$

Using (6) and (3), we obtain

$$G_{in} = -\frac{(W_2 + W_3)}{1/2\,|V_1|^2\, G_c} \tag{7}$$

Using (4), this can be written as

$$G_{in} = -\left\{\frac{\frac{\omega_1}{\omega_3} W_3 - \frac{\omega_1}{\omega_2} W_2}{1/2\,|V_1|^2}\right\} \tag{8}$$

In Fig. 2, both conversion gain and input conductance are plotted as a function of (W_2/W_3). To accurately plot the input conductance, one needs to know the actual relation between W_2, W_3 and $|V_1|^2$ as well as the manner in which (W_2/W_3) is varied. For the sake of simplicity, it has been assumed in plotting the input conductance that $(W_2+W_3)/(\frac{1}{2}|V_1|^2)$ is kept constant while W_2/W_3 is varied.

As seen from Fig. 2, the particular mode of operation depends on the power ratio W_2/W_3 which in turn is decided by the relative loading of the two sidebands. An upper sideband up-converter ($W_2/W_3 = 0$) exhibits maximum positive input conductance but its conversion gain is limited to a maximum value of ω_3/ω_1. However, the conversion gain can be increased by also providing a loading for the lower sideband. This reduces the input conductance by the amount of negative conductance the lower sideband reflects at the input. As one increases

this loading, a point is reached at which it equals the upper sideband loading. As noted subsequently, this point corresponds to $W_2/W_3=(\omega_2/\omega_3)^2$. This operation known as the double sideband up-conversion has a theoretical conversion gain of $1+(\omega_p/\omega_1)^2$, (4), and still has a positive input conductance although much smaller than that of an upper sideband up-converter. Furthermore, favoring of the lower sideband approaches the critical point mentioned previously at which point the input conductance becomes zero. This happens when $W_2/W_3=\omega_2/\omega_3$. Theoretical conversion gain of this type of operation is infinite owing to its infinite input impedance and, hence, this mode of operation is similar to that of a vacuum tube triode amplifier. Any further increase in lower sideband loading will result in a negative input conductance which reaches a maximum value as $W_2/W_3\rightarrow\infty$. This point of operation corresponds to a lower sideband up-converter.

The aforementioned modes of operation are summarized in Table I.

TABLE I

W_2/W_3	G_c	G_{in} (arbitrary units)	Mode of operation
0	ω_3/ω_1	ω_1/ω_3	Upper sideband up-converter
$(\omega_2/\omega_3)^2$	$1+(\omega_p/\omega_1)^2$	$(1+(\omega_p/\omega_1)^2)^{-1}$	Double sideband up-converter
(ω_2/ω_3)	∞	0	Double sideband up-converter (triode type)
∞	$-(\omega_2/\omega_1)$	$-(\omega_1/\omega_2)$	Lower sideband up-converter

Devices Using a Nonlinear Capacitor

Although the general energy relations of Manley and Rowe [8] give some insight into the basic modes of operations of a parametric up-converter, more detailed information can only be obtained with further knowledge on the nature of the nonlinear element involved and its associated circuitry. In this paper, we consider a nonlinear capacitor such as a reverse-biased junction diode as the element used for the parametric conversion.

A nonlinear capacitor, for small signal amplitudes, under the application of sinusoidal pumping may be represented by an equivalent time-varying capacitance. As long as the diode does not draw any appreciable current in either direction, this time-varying capacitance may be written as

$$C(t) = C_0 + 2C_1 \operatorname{Cos} \omega_p t + 2C_2 \operatorname{Cos} 2\omega_p t + \cdots \quad (9)$$

where $2C_1$ and $2C_2$ are the amplitudes of the capacitance variations at the fundamental and second harmonic of the pump frequency. These coefficients, for a given nonlinear $Q-V$ characteristic and dc bias, depend on the pump level used in a specific case. The ratios (C_1/C_0), (C_2/C_0) etc. have been graphed by Blackwell and Kotzebue [9] as a function of the normalized excitation level.

Low-Level Pumping

When the level of excitation is low, we need consider only the average capacitance C_0 and the fundamental capacitance variation C_1 in (9). Under these conditions, the currents (Fig. 1) flowing at the lower and upper sideband frequencies [10] are given by

$$I_2 = j\omega_2 C_1 V_1^{*1} \quad (10)$$

$$I_3 = j\omega_3 C_1 V_1 \quad (11)$$

The energy dissipated in each of the sideband loads is

$$W_2 = -1/2 \left| I_2 \right|^2 \text{Re. } 1/Y_2 \quad (12)$$

and

$$W_3 = -1/2 \left| I_3 \right|^2 \text{Re. } 1/Y_3 \quad (13)$$

where Y_2 and Y_3 now include the average incremental capacitance C_0. Substituting (10) and (11) into (12) and (13), the ratio of energy dissipated in the lower sideband to that in the upper sideband may be determined as

$$W_2/W_3 = (\omega_2/\omega_3)^2 \frac{\text{Re. } 1/Y_2}{\text{Re. } 1/Y_3} \quad (14)$$

After substitution in (8), expressions (12) and (13), the general expression for the input conductance of a double sideband up-converter (for low-pump levels) is

$$G_{in(s)} = \omega_1 C_1^2(\omega_3 \text{ Re. } 1/Y_3 - \omega_2 \text{ Re. } 1/Y_2) \quad (15)$$

The double sideband up-converter with equal sideband loading corresponds to the case where Re. $1/Y_2=$ Re. $1/Y_3$, and it is seen from (14) that $(W_2/W_3)=(\omega_2/\omega_3)^2$ in this case, as was mentioned in the foregoing.

High-Level Pumping

As indicated previously, when the pump level is low enough so that C_2 may be neglected, the only coupling that exists between the lower and upper sideband, ω_2 and ω_3, is through the signal ω_1 and the fundamental capacitance variation C_1. However, as the pump level increases, the presence of C_2 introduces a direct coupling between ω_2 and ω_3. As shown by Rowe [10], the currents flowing at ω_2 and ω_3 now are given by the following relations:

$$I_2 = j\omega_2 C_1 V_1^* + j\omega_2 C_2 V_3^* \quad (16)$$

$$I_3 = j\omega_3 C_1 V_1 + j\omega_3 C_2 V_2^* \quad (17)$$

Referring to Fig. 1, the terminal relations that exist at the lower and upper sideband ports are $V_2=-I_2/Y_2$ and $V_3=-I_3/Y_3$.

[1] * Indicates complex conjugate.

It is now convenient to define two modified sideband admittances, such as

$$Y_3' = Y_3 - j\omega_3 C_2 \tag{18}$$

$$Y_2' = Y_2 - j\omega_2 C_2 \tag{19}$$

Substituting the terminal relations in (16) and (17), and solving for I_2 and I_3, we find

$$I_2 = \frac{j\omega_2 C_1 V_1^*}{\left(1 - \frac{\omega_2\omega_3 C_2^2}{Y_2 Y_3^*}\right)} \cdot \frac{Y_3'^*}{Y_3^*} \tag{20}$$

$$I_3 = \frac{j\omega_3 C_1 V_1}{\left(1 - \frac{\omega_2\omega_3 C_2^2}{Y_2^* Y_3}\right)} \cdot \frac{Y_2'^*}{Y_2^*} \tag{21}$$

Substituting (20) and (21) into (12) and (13), we find after some algebraic manipulation that

$$\frac{W_2}{W_3} = \left(\frac{\omega_2}{\omega_3}\right)^2 \cdot \frac{\text{Re. } 1/Y_2'}{\text{Re. } 1/Y_3'} \tag{22}$$

Comparison of (22) and (14) reveals that the energy ratio W_2/W_3 is the same except that, for large pump levels, Y_2 and Y_3 are replaced by Y_2' and Y_3', respectively.

Now, as indicated earlier, Y_2 and Y_3 include the average incremental capacitance C_0. From (18) and (19), we know that Y_2' and Y_3' include the capacitance C_0–C_2. This, however, is just the diode large signal capacitance C_{ls} seen by the pump [11]. The physical significance of this is that the sidebands and pump always see the same average diode capacitance.

It remains for us to evaluate the input conductance for high pump levels. This may be done by again using (20), (21), (12), and (13), and substituting into (8). After a somewhat tedious procedure, the result is found to be

$$G_{in(l)} = \frac{1}{\left|1 - \frac{j\omega_3 C_2}{Y_3'^*} + \frac{j\omega_2 C_2}{Y_2'}\right|^2} \cdot \omega_1 C_1^2(\omega_3 \text{ Re. } 1/Y_3' - \omega_2 \text{ Re. } 1/Y_2') \tag{23}$$

This expression for the input conductance for high-pump levels differs from that for low-pump levels (15) by the substitution of Y_3' and Y_2' in place of Y_3 and Y_2, respectively, as discussed before and by a factor

$$\beta = \frac{1}{\left|1 - \frac{j\omega_3 C_2}{Y_3'^*} + \frac{j\omega_2 C_2}{Y_2'}\right|^2} \tag{24}$$

This "feedback" factor β arises from the coupling between the sidebands through C_2 which establishes a feedback loop through the amplifier.

Equation (23) can be written as

$$G_{in(l)} = \beta w_1 C_1^2(\omega_3 \text{ Re. } 1/Y_3' - \omega_2 \text{ Re. } 1/Y_2') \tag{25}$$

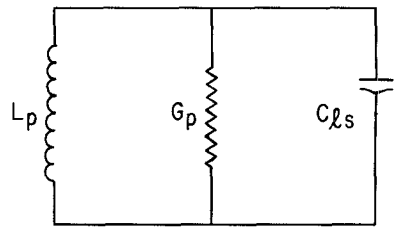

Fig. 3. Equivalent circuit of a varactor diode configuration.

Analysis of a Four-Frequency Up-Converter Using a Single Resonant Circuit for Both Idlers and Pump

The varactor diode configuration used in our experiments may be represented by an equivalent circuit as shown in Fig. 3 where L_p is the inductance, G_p is the effective shunt conductance, and C_{ls} is large signal capacitance of the diode. As pointed out earlier, such a circuit, tuned to the pump frequency and also acting as a termination for both sidebands, provides flexibility in controlling the gain and bandwidth of diode up-converters. Since we are particularly interested in the behavior of input conductance as a function of the deviation of pump frequency from resonant frequency of the circuit, it is convenient to define the following parameters:

$$\delta = 2\frac{\Delta\omega_p}{\omega_p} Q_p = 2\frac{\omega\Delta_p}{\Omega_p} \tag{26}$$

and

$$\delta' = 2\frac{\omega_1}{\omega_p} Q_p = 2\frac{\omega_1}{\Omega_p} \tag{27}$$

where

ω_1 is the signal frequency
ω_p is the pump circuit resonant frequency
Q_p is the quality factor of the pump circuit (measured at low-pump level)
$\Delta\omega_p$ is the deviation of pump from resonant frequency
Ω_p is the radian bandwidth of the pump circuit ($\Omega_p = \omega_p/Q_p$)

If $\Delta\omega_p/\omega_p \ll 1$, the admittances offered by this circuit to the two sidebands can be written as

$$Y_3 = G_p(1 + j\delta + j\delta') \tag{28}$$

$$Y_2 = G_p(1 + j\delta - j\delta') \tag{29}$$

Low-Level Pumping

In the case of low-pump levels, owing to the absence of C_2, the sidebands see the average incremental capacitance C_0 which is just equal to C_{ls}. It can be shown from (15), using (28) and (29), that the input conductance for small pump levels is

$$G_{in(s)} = \frac{-4\omega_p\omega_1 C_1^2}{G_p} \cdot \frac{\delta\delta'\left(1 - \frac{1}{4Q\delta}(1 + \delta^2 + \delta'^2)\right)}{(1 + \delta^2 - \delta'^2)^2 + 4\delta'^2} \tag{30}$$

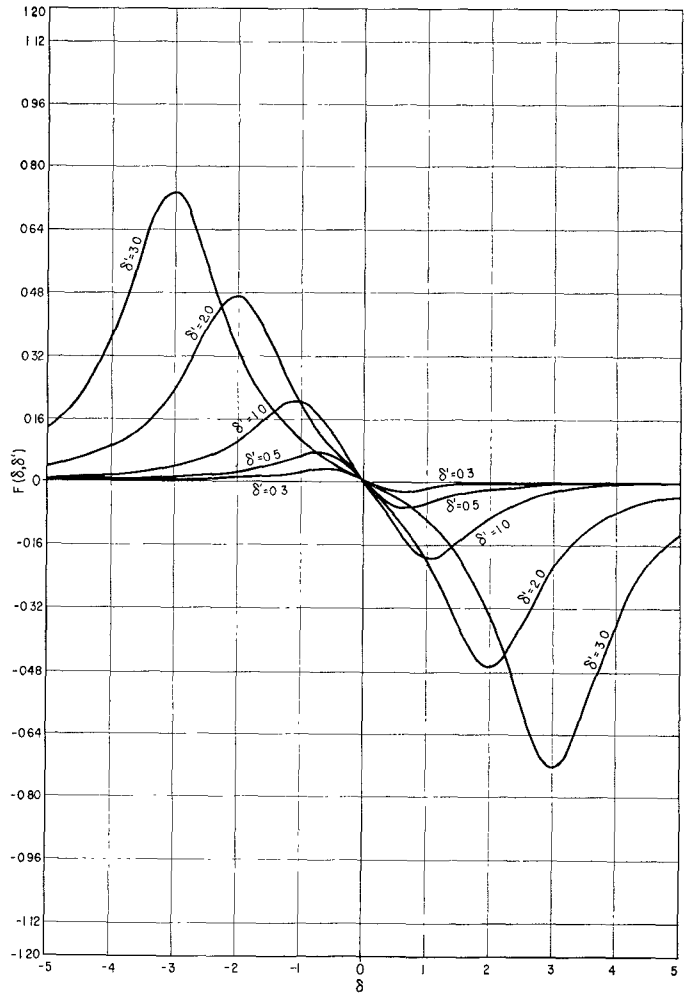

Fig. 4. Normalized input conductance for small level pumping $F(\delta, \delta')$, as a function of pump frequency deviation (δ) for various values of input frequency (δ').

For the sake of simplicity, we assume δ is restricted to a range $4Q\delta \gg 1$, thereby excluding a small region around $\delta = 0$. Then, (30) can be simplified to read:

$$G_{in(s)} = 2\omega_p C_{ls} \left(\frac{C_1}{C_{ls}}\right) F(\delta, \delta') \tag{31}$$

and

$$F(\delta, \delta') = \frac{-\delta\delta'^2}{(1 + \delta^2 - \delta'^2)^2 + 4\delta'^2} \tag{32}$$

The expression $F(\delta, \delta')$ represents the normalized input conductance as a function of deviation of pump and signal frequency. The values of $F(\delta, \delta')$ are plotted as a function of δ for various values of the parameter δ' in Fig. 4. In accordance with our expectations, the curves are antisymmetrical since detuning of pump away from center frequency on either side favors one sideband with respect to the other by the same amount. Thus, the input conductance for the same amount of detuning is of same magnitude but of opposite sign.

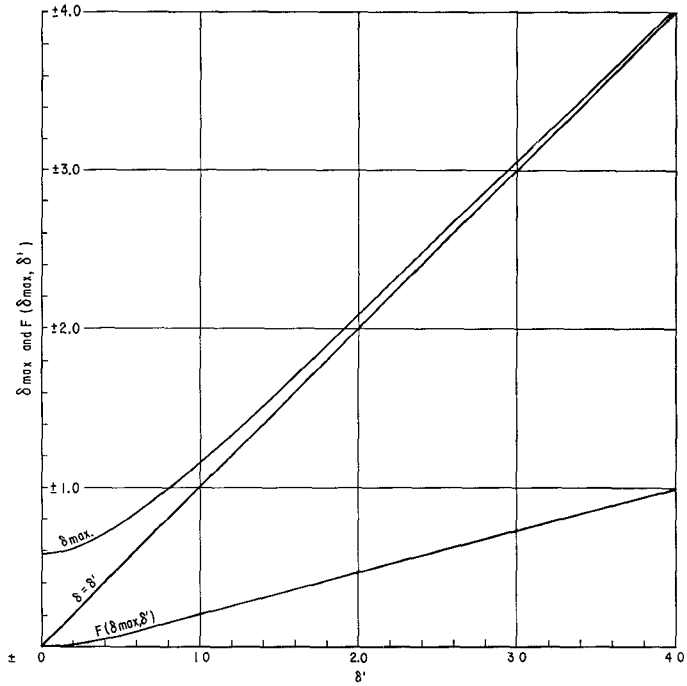

Fig. 5. Maximum input conductance and corresponding pump frequency deviation as a function of input frequency.

The values of δ, for which $F(\delta, \delta')$ is maximum, are found by differentiation of (32), as

$$\delta_{max} = \pm\frac{1}{\sqrt{3}} \left[\sqrt{(1-\delta'^2)^2 + 3(1+\delta'^2)^2} - (1-\delta'^2)\right]^{1/2} \tag{33}$$

and this relation is plotted in Fig. 5.

When $\omega_1 \ll \omega_p$, i.e., $\delta' \ll 1$,

$$\delta_{max} = \pm\frac{1}{\sqrt{3}} \quad \text{and} \quad F(\delta, \delta') = \frac{3\sqrt{3}}{16}\delta'^2 \tag{34}$$

However, if $\delta' \gg 1$,

$$\delta_{max} = \pm\delta' \quad \text{and} \quad F(\delta, \delta') = \frac{\delta}{4} \tag{35}$$

This behavior may be verified from the graphs of Fig. 4. As seen from Fig. 5, the δ_{max} asymptotically approaches δ' for values of $\delta' \gg 1$. This is as to be expected, since for large values of δ' and δ, the operation of the device is effectively determined by one sideband only.

High-Level Pumping

As stated beforehand, we can write the admittances offered to the sidebands by the resonant circuit as

$$Y_3' = G_p(1 + j\delta + j\delta') \tag{36}$$

$$Y_2' = G_p(1 + j\delta - j\delta') \tag{37}$$

Y_3' and Y_2', however, now include the large signal capacitance C_{ls} rather than C_0, as indicated previously.

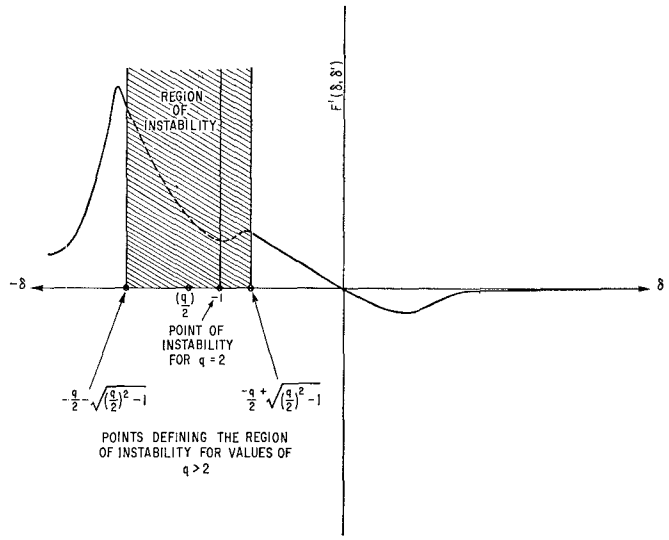

Fig. 6. Instability region at high-pump levels.

Substituting (36) and (37) into (24) for β, it may be shown that

$$\beta = \frac{(1 - j\delta - j\delta')(1 + \delta j - j\delta')}{(1 + \delta^2 - \delta'^2) - q\left(\frac{\delta'^2}{2Q_p} - \delta\right) - j\delta'\left(2 + \frac{q}{2Q_p}\right)} \tag{38}$$

where

$$q = \frac{2\omega_p C_2}{G_p} = 2Q_p\left(\frac{C_2}{C_{ls}}\right)$$

Now, making the following assumptions:

$$q \ll 4Q_p \tag{38a}$$

and

$$\frac{\delta'^2}{2Q_p} \ll \delta \tag{38b}$$

Equation (38) can be reduced to

$$\beta = \frac{(1 + \delta^2 - \delta'^2)^2 + 4\delta'^2}{(1 + \delta^2 - \delta'^2 + q\delta)^2 + 4\delta'^2} \tag{39}$$

Assumption (38a) restricts the value of C_2 to much less than $2C_{ls}$ which generally is true. Assumption (38b) places another lower bound on the deviation of the pump, i.e., $4Q_p\delta \gg 2\delta'^2$. This, however, does not seriously affect the useful range in which (39) is valid. If, as before, it is also assumed that $4Q_p\delta \gg 1$, then using (39) in combination with (25) and (32), the input conductance for high-pump levels can be written as

$$G_{\text{in}(l)} = 2\omega_p C_{ls}\left(\frac{C_1}{C_{ls}}\right)^2 F'(\delta, \delta') \tag{40}$$

where

$$F'(\delta, \delta') = \frac{-\delta\delta'^2}{(1 + \delta^2 - \delta'^2 + q\delta)^2 + 4\delta'^2} \tag{41}$$

Equation (41) represents a normalized input conductance for high-pump levels.

As seen from (41), $F'(\delta, \delta')$ becomes identical to $F(\delta, \delta')$ for $q = 0$, i.e., low level pumping.

Ferroresonant Effect

Examination of (41) shows an anomalous behavior of the input conductance for zero signal frequency. In general, the input conductance equals zero in this case except for two well-defined singular values of δ, where the normalized input conductance becomes finite and of value $-\delta/4$. The values of δ at which this effect occurs are given by the equation

$$(1 + \delta^2 + q\delta)^2 = 0 \tag{42}$$

or

$$\delta = \frac{-q}{2} \pm \sqrt{\left(\frac{q}{2}\right)^2 - 1} \tag{43}$$

Now, it is recognized that these values of δ are the same at which the ferroresonant effect sets in [12]. This effect, also called the "jump effect," is caused by regenerative action due to increase of large signal capacitance with pump level. It also may be thought of as degenerate parametric action by which the pump is coupled to itself through the second harmonic capacitance variation C_2 [12]. This is observed in practice by a switching (jumping) of the current to a different level of operation outside the range (43). Thus, a region of δ between the two points given by (43) is not accessible to experimental investigation. This region of instability is indicated in Fig. 6. It is seen by inspection of (43) that the ferroresonant effect does not occur for values of $q < 2$.

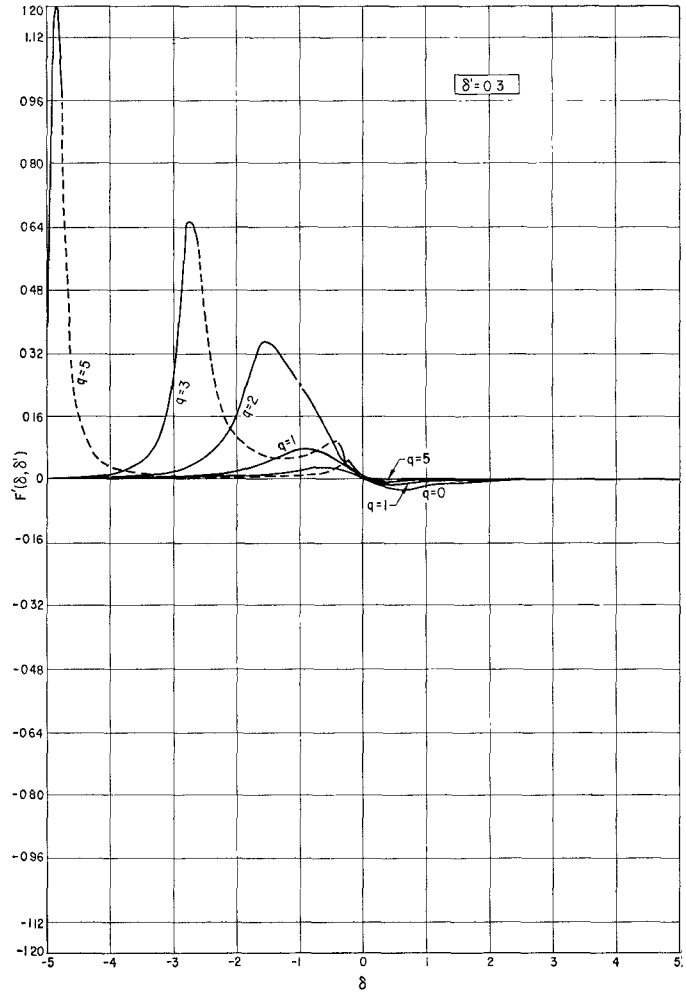

Fig. 7. Normalized input conductance as a function of pump deviation for various values of input frequency (δ'), and second harmonic capacitance variation (q).

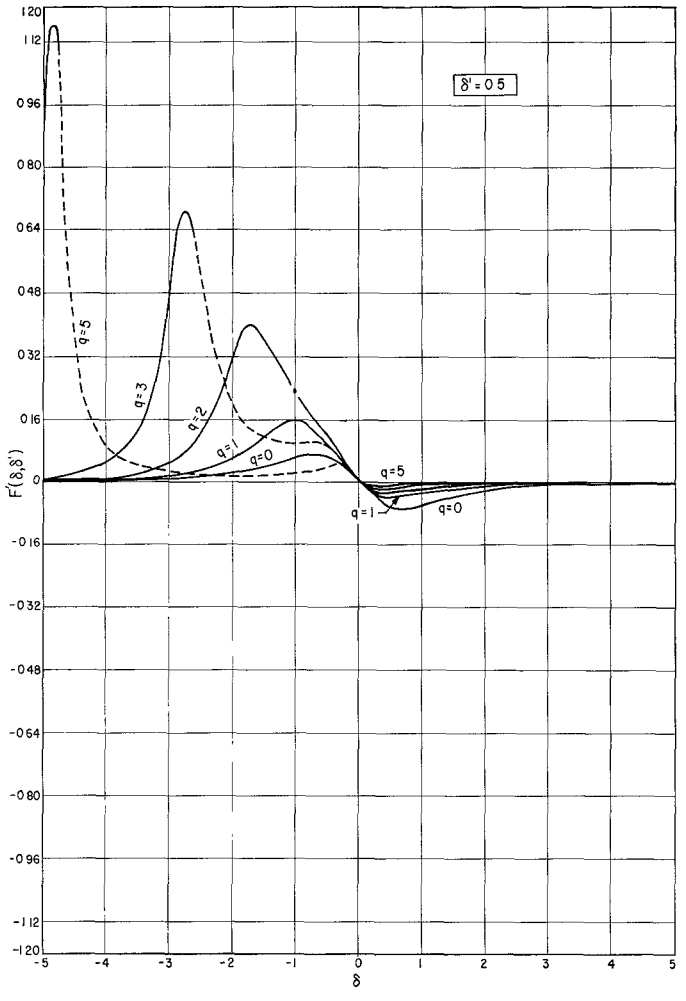

Fig. 8. Normalized input conductance as a function of pump deviation for various values of input frequency (δ'), and second harmonic capacitance variation (q).

Numerical Calculations

To examine the behavior of normalized input conductance for high pump levels when the pump is detuned from the resonant frequency of the circuit, values of $F'(\delta, \delta')$ (41) were computed using an IBM 1620 Computer. The numerical results are graphed in Figs. 7 to 11, pp. 102–104. For a given value of δ', $F'(\delta, \delta')$ is plotted as a function of δ, with q as the parameter. As pointed out earlier, when $q=0$, $F'(\delta, \delta')$ is antisymmetrical for all values of δ'. In this case, the maxima of $F'(\delta, \delta')$ occur at equal values of δ on either side of the resonant frequency and are equal and opposite in magnitude. However, if q is increased, the positive maximum of $F'(\delta, \delta')$ increases and occurs at a higher negative value of deviation ratio δ. On the other hand, the negative maximum decreases and occurs at a smaller value of positive deviation ratio. This trend continues until q reaches a critical value at which two maxima occur in the negative δ region with the smaller maximum occurring nearer the origin ($\delta=0$). Further increase in q results in increase in value of the large maximum, whereas the value of smaller maximum is decreased. Also, while the large maximum is displaced further away from the origin, the other maximum moves closer to it. However, for $q<2$, there is only one maximum on either side of the resonant frequency and, as seen, the critical value of q is always greater than two for all values of δ'.

It is noted by examination of the graphs (Figs. 7 to 11) that the critical value of q at which multiple peaks appear increases with δ'. This critical value of q is calculated by means of a method outlined in Appendix I, and is plotted in Fig. 12 as a function of δ'.

In each case, the region of instability is indicated by the dotted section of the curve (Figs. 7 to 11) and, as stated previously, the theoretical values plotted in this region have no practical significance since there cannot be any measurements made here.

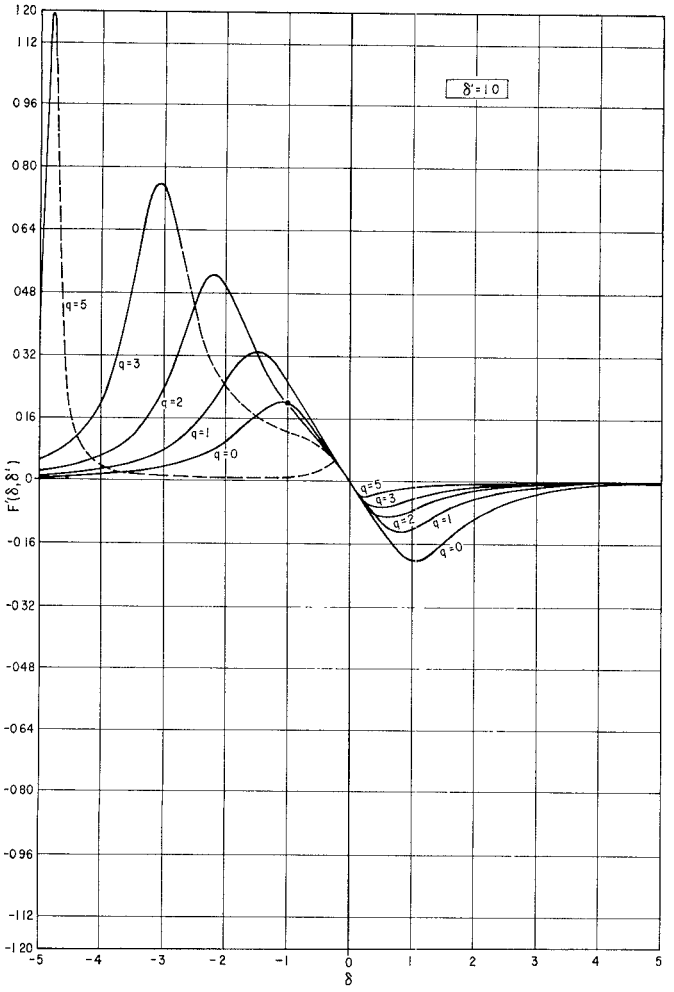

Fig. 9. Normalized input conductance as a function of pump deviation for various values of input frequency (δ'), and second harmonic capacitance variation (q).

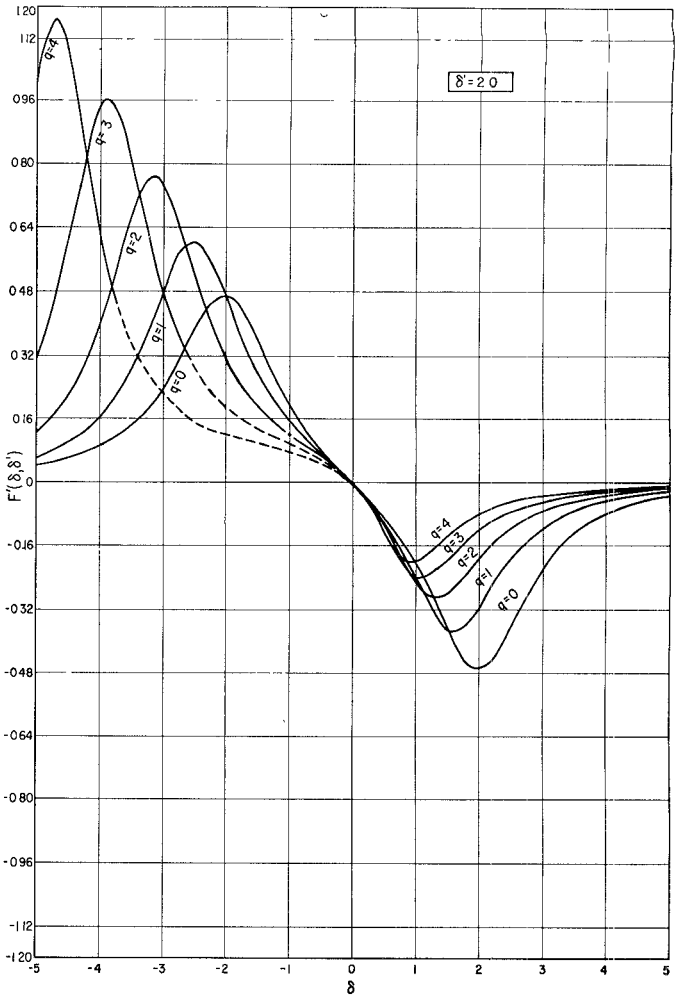

Fig. 10. Normalized input conductance as a function of pump deviation for various values of input frequency (δ'), and second harmonic capacitance variation (q).

Experimental Results

Figure 13 shows a simplified schematic diagram of the experimental arrangement. The pump circuit consists of the balanced arrangement of C_1, C_d, L_1, and L_d. R_d represents the loss resistance of the varactor diode. C_d represents the diode capacity, and L_d includes the lead inductance of the diode. C_1 and L_1 are made approximately equal to C_d and L_d. This balanced arrangement is convenient because the signal can be coupled to the diode through a simple RF choke L_c, thereby avoiding extraneous capacitive loading. The pump circuit uses a graded junction diode (MA450 C) and resonates at 1895 Mc/s (for low pump levels). The measured bandwidth is 140 Mc/s. The signal circuit L_{in}, C_{in}, resonates at 42.5 Mc/s. The loading of this signal circuit can be varied by adjusting the coupling of the source of the output circuit, and by tapping at appropriate points on coil L_{in}. To facilitate detection, the input signal is modulated at 1000 c/s. The output circuit consists of an RF amplifier followed by a detector and a 1000 c/s tuned amplifier. During the small signal measurement, both the incident and the reflected pump power are monitored, and the incident power is kept constant.

For a given setting of the pump frequency, the output signal is measured with the pump on and off. Depending upon the measured values of gain or loss, as the case may be, the ratio of reflected input conductance $G_{in(s)}$ to the passive circuit conductance G_s may be computed. Figure 14 shows the ratio $G_{in(s)}/G_s$ as a function of pump frequency (triangles). Inspection of these experimental points shows a lack of the expected symmetry. This is explained as follows:

Sideband currents are generated in the diode in proportion to the pump voltage across the diode capacity. Sideband voltages across the same capacity then are determined by the impedance of the antiresonant circuit which is formed with the other elements. Because

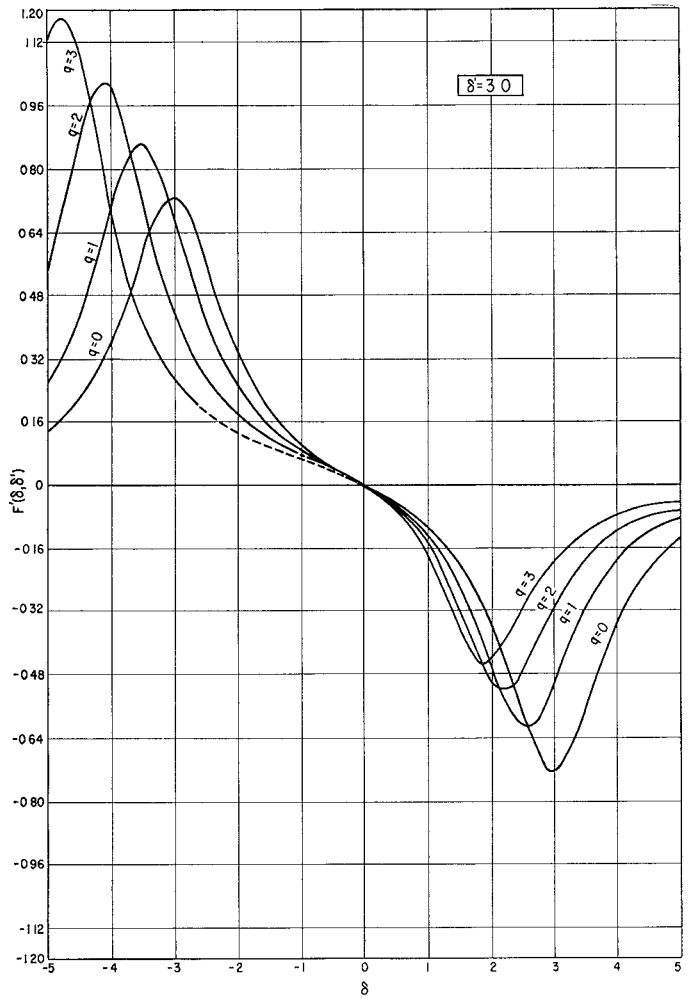

Fig. 11. Normalized input conductance as a function of pump deviation for various values of input frequency (δ'), and second harmonic capacitance variation (q).

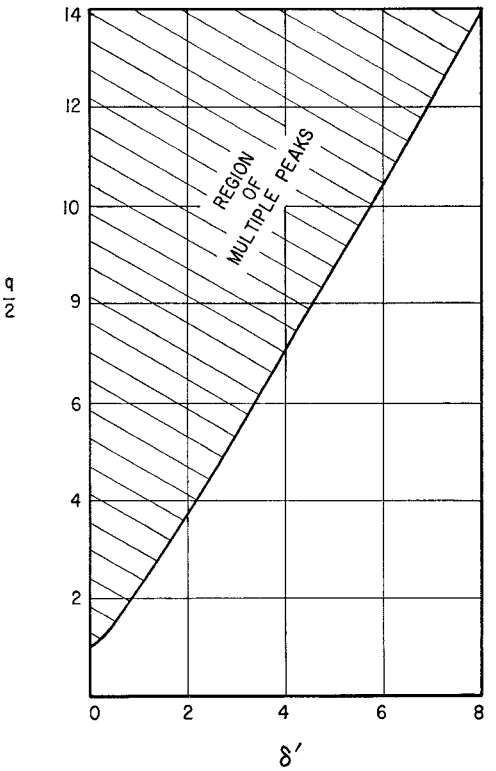

Fig. 12. Region of multiple peaks defined by second harmonic capacitance variation (q) and input frequency (δ').

this is a low-Q circuit, the impedance maximum of the antiresonant circuit does not coincide with the impedance minimum of the resonant circuit seen by the pump drive; the latter resonant frequency is about 0.5 per cent higher, thus enhancing the observed effects on the high-frequency side of the antiresonance by stronger pumping.

In order to compare theory and experiment, we computed the normalized input conductance for low-level pumping (32) using the measured values of bandwidth and input frequency. To correct for asymmetry mentioned before, the computed values were multiplied by the normalized response of the pump circuit. Finally, a constant multiplier was chosen to best fit the experimental points. The result is indicated by the solid line in Fig. 14 which shows good agreement with the measured values. From the value of the constant multiplier and the measured value of the passive input conductance, we calculated the value of C_1/C_{ls} at the point of resonance (31). The value of $C_1/C_{ls}=0.06$ obtained in this was in good agreement with the one computed from the measured pump amplitude and dc bias on the diode [11].

The same measurements were repeated for high pump levels. In this case, however, it was possible to keep the voltage level across the diode constant by maintaining a constant direct current of about one-half μA through the diode. Figure 15 illustrates the measured ratio $G_{in(l)}/G_s$ as a function of pump frequency. In order to compute the theoretical curve, it is necessary to know the exact value of q corresponding to this pump level. We can determine this value from observation of the ferroresonant instability. For this purpose, we detuned the pump until the instability occurred. From the measured value of the deviation δ at this point, we calculated q, using (42). The value obtained corresponds to $C_2/C_{ls}=0.2$ which again shows good agreement with the computed value for full pumping [9].

In the final calculation of the relative input conductance (40), we used this value $C_2/C_{ls}=0.2$ together with the corresponding value $C_1/C_{ls}=0.36$ [9], and the measured loss conductance. The final results are plotted as a solid line in Fig. 15, the dashed part representing the unstable region. As indicated, there is very good agreement with the measured values. For comparison, we also plotted the same curve with $C_2=0$ (dashed line) in Fig. 15, showing clearly the effect of second harmonic capacitance variation.

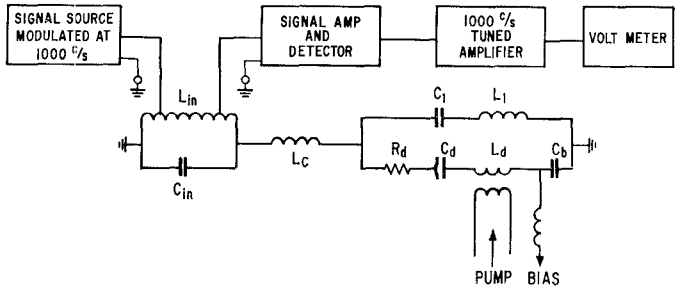

Fig. 13. Experimental setup.

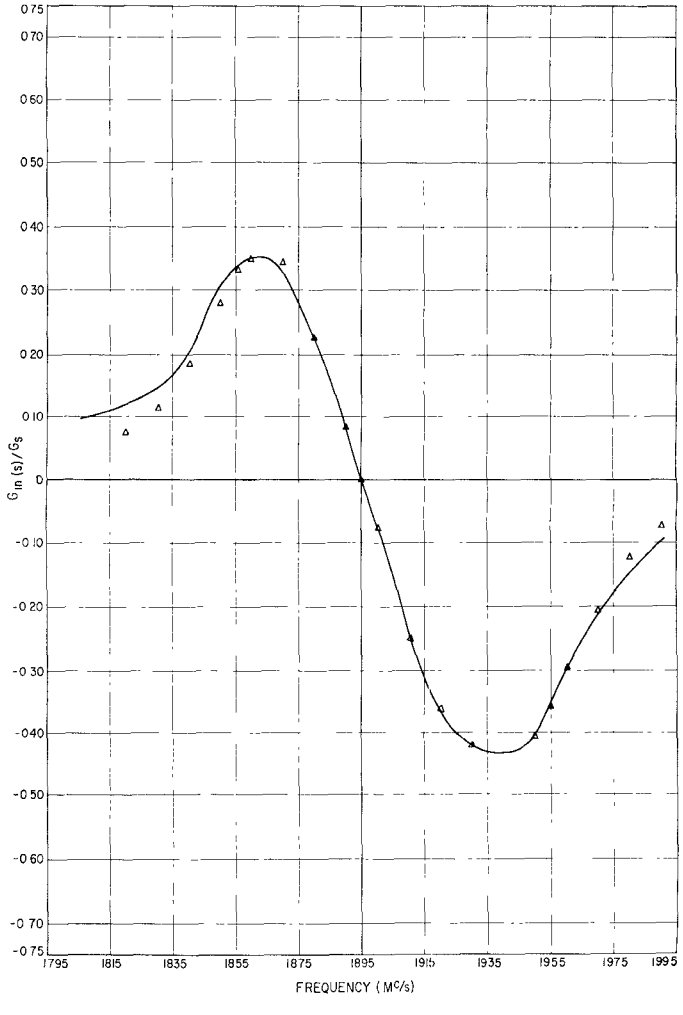

Fig. 14. Measured (triangles) and calculated (solid line) relative input conductance as a function of pump frequency for small pump levels.

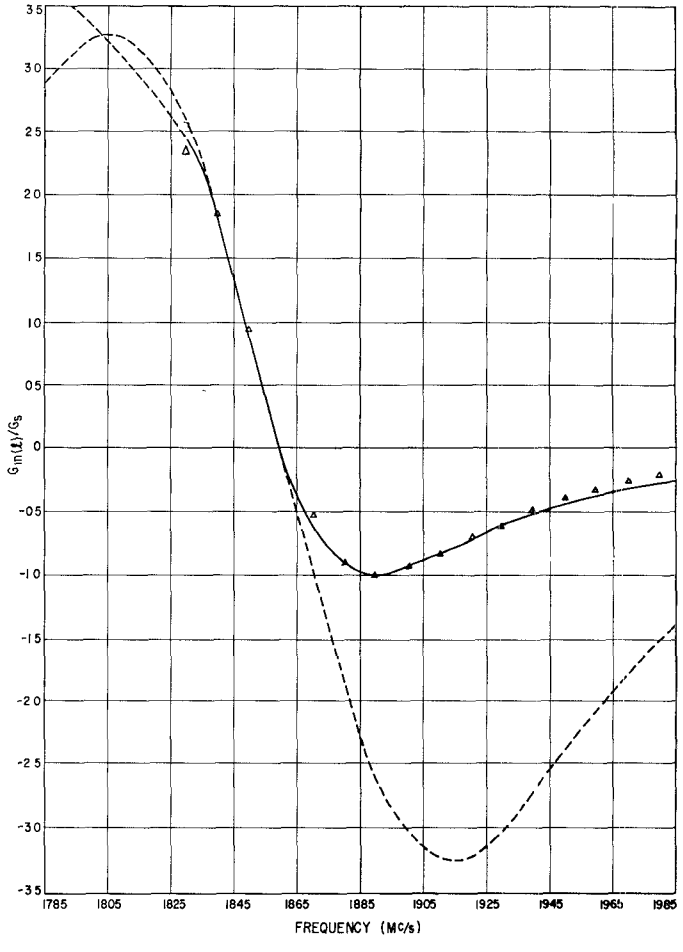

Fig. 15. Measured (triangles) and calculated (solid line) relative input conductance as a function of pump frequency for high-pump levels.

Conclusion

The simple circuit investigated here could well lend itself to a variety of operating conditions between those of an upper sideband up-converter and a lower sideband up-converter. Indeed, the analysis shows a wide range of possible values of input conductance dependent on pump detuning. It also shows, however, the serious effects that occur at high pump level due to second harmonic capacitance variation. This, on one hand, causes the ferro resonant or jump effect which restricts the operating range; on the other hand, it causes a severe asymmetry in the curve which depicts input conductance vs. pump detuning. This asymmetry reduces the maximum available negative conductance. In pointing out these features, and in deriving some simple analytical expressions checked by experiments, it is hoped that this analysis may be of use in the design of this class of four-frequency parametric devices.

Appendix I

The function considered here (41) is given by

$$F'(\delta, \delta') = \frac{-\delta\delta'^2}{(1+\delta^2+\delta'^2+q\delta)^2+4\delta'^2}$$

In order to find the extrema of $F'(\delta, \delta')$ as a function of δ, we set $dF'/d\delta = 0$, and find

$$G(\delta, \delta') = -(1+\delta^2-\delta'^2+q\delta)^2 + 4\delta\left(\frac{q}{2}+\delta\right)(1+\delta^2-\delta'^2+q\delta) - 4\delta'^2 = 0 \quad (44)$$

or

$$G(\delta, \delta') = 3\delta^4 + 4q\delta^3 + \delta^2[q^2+2(1-\delta'^2)] - (1+\delta'^2)^2 = 0 \quad (45)$$

It is seen that the function $G(\delta, \delta')$ has the following properties:

$$G(\delta, \delta') > 0 \qquad \text{for } \delta \to \pm\infty \quad (46)$$

$$G(\delta, \delta') < 0 \qquad \text{for } \delta = 0 \text{ and } \delta = -q/2 \quad (47)$$

Next, we consider the extrema of $G(\delta, \delta')$ itself. Again, differentiating with respect to δ and setting $dG(\delta, \delta')/d\delta = 0$, we find

$$H(\delta, \delta') = 6\delta^3 + 6q\delta^2 + \delta[q^2+2(1-\delta'^2)] = 0 \quad (48)$$

Hence, the roots of $H(\delta, \delta')$ are found to be

$$\delta_1 = 0 \quad (49)$$

$$\delta_{2,3} = -q/2 \pm \frac{1}{\sqrt{3}}\sqrt{(q/2)^2-(1-\delta'^2)} \quad (50)$$

Now, if $(q/2)^2 < (1-\delta'^2)$, then $H(\delta, \delta')$ has only one real root, i.e., $\delta = \delta_1$. Accordingly, $G(\delta, \delta')$ has only one extremum at this point. From (46) and (47), it follows that this is a negative minimum. Therefore, it follows with (46) that $G(\delta, \delta')$ has but two real roots corresponding to $F'(\delta, \delta')$ having only two peaks.

However, if $(q/2)^2 > (1-\delta'^2)$, the function $H(\delta, \delta')$ has three real roots, one of which equals zero, the other two being negative. In order of increasing magnitude, they are

$$\delta_1 = 0$$

$$\delta_2 = -(q/2) + \frac{1}{\sqrt{3}}\sqrt{(q/2)^2-(1-\delta'^2)}$$

$$\delta_3 = -(q/2) - \frac{1}{\sqrt{3}}\sqrt{(q/2)^2-(1-\delta'^2)}$$

The function $G(\delta, \delta')$, therefore, has three extrema at these points. From (46) and (47), it now may be deduced that δ_1 and δ_3 correspond to negative minima of $G(\delta, \delta')$ for all values of q and δ'. The maximum at δ_2 may be either positive or negative depending on the values of q and δ'. It is evident that these cases correspond to $G(\delta, \delta')$ having four and two real roots, respectively. This in turn corresponds to $F'(\delta, \delta')$ having either four or two peaks. Thus, the condition for multiple peaks corresponds to

$$G(\delta_2, \delta') \geq 0 \quad (51)$$

Making the following substitutions:

$$Y = (\delta + q/2) \quad (52)$$

$$X^2 = (q/2)^2 - (1-\delta'^2) \quad (53)$$

$G(\delta, \delta')$ can be written as

$$G(\delta,\delta') = \left(\frac{q}{2}\right)^2 + \left(\frac{q}{2}\right)\left[\frac{2X^3}{3\sqrt{3}} - \left(Y-\frac{X}{\sqrt{3}}\right)\left(Y+\frac{2X}{\sqrt{3}}\right)\right] - \left[\frac{X^4}{3}+X^2+1\right] + \frac{1}{12}[X^2-3Y^2]^2 \quad (54)$$

Substituting the correct value of Y corresponding to $\delta = \delta_2$, i.e., $Y = X/\sqrt{3}$, the condition for multiple peaks (51) may be written as

$$\left(\frac{q}{2}\right)^2 + \left(\frac{q}{2}\right)\frac{2X^3}{3\sqrt{3}} - \left[\frac{X^4}{3}+X^2+1\right] \geq 0 \quad (55)$$

Solving for the equality of (55)

$$\frac{q}{2} = -\frac{X^3}{3\sqrt{3}} + \sqrt{\left(\frac{X^2}{3}+1\right)^3} \quad (56)$$

Using (56) together with (53), the required value of $(q/2)$ to just cause multiple peaks for a given δ' has been plotted in Fig. 12.

References

[1] Adams, D. K., An analysis of four-frequency nonlinear reactance circuits, *IRE Trans. on Microwave Theory and Techniques*, vol MTT-8, May 1960, pp 274–283.

[2] Jones, E. M. T., and J. S. Honda, A low noise up-converter parametric amplifier, *1959 WESCON Conv. Rec.*, pt. 1, pp 99–107.

[3] Luksch, J. A., E. W. Matthews, and G. A. Verwys, Design and operation of four-frequency parametric up-converters, *IRE Trans. on Microwave Theory and Techniques*, vol MTT-9, Jan 1961, pp 44–52.

[4] Anderson, D. B., and J. C. Aukland, A general catalog of gain, bandwidth and noise temperature expressions for four-frequency parametric devices, *IEEE Trans. on Electron Devices*, vol ED-10, Jan 1963, pp 13–30.

[5] Boyd, C. R., A general approach to the evaluation of n-frequency parametric mixers, *Proc. NEC*, vol 16, Oct 1960, pp 472–479.

[6] Adams, D. K., The optimum design of wide band phase shift amplifiers, *Proc. NEC*, vol 19, 1963, pp 453–455.

[7] Brett, H., F. A. Brand, and W. G. Matthei, A varactor diode parametric standing-wave amplifier, *Proc. IRE*, vol 49, Feb 1961, pp 509–510.

[8] Manley, J. M, and H. E. Rowe, Some general properties of nonlinear elements—pt 1. General energy relations, *Proc IRE*, vol 44, Jul 1956, pp 904–913.

[9] Blackwell, L. A., and K. L. Kotzebue, *Semiconductor Diode Parametric Amplifiers*. Englewood Cliffs, N. J.: Prentice-Hall, 1961, pp 127–130.

[10] Rowe, H. E., Some general properties of nonlinear elements—pt 2. Small signal theory, *Proc. IRE*, vol 46, May 1958, pp 850–860.

[11] Korpel, A., and V. Ramaswamy, Some useful relations between nonlinear capacitance parameters, *Proc. IEEE (Correspondence)*, vol 51, Jul 1963, pp 1044–1045.

[12] Korpel, A., and V. Ramaswamy, Ferroresonant effect caused by nonlinear capacitors, *Proc. IEEE (Correspondence)*, vol 52, Jan 1964, p 82.